

Pressure-tuned magnetic interactions in honeycomb Kitaev materials

Ravi Yadav,¹ Stephan Rachel,² Liviu Hozoi,¹ Jeroen van den Brink,^{1,3} and George Jackeli^{4,5,*}

¹*Institute for Theoretical Solid State Physics, IFW Dresden, Helmholtzstr. 20, 01069 Dresden, Germany*

²*School of Physics, University of Melbourne, Parkville, VIC 3010, Australia*

³*Department of Physics, Technical University Dresden, 01062 Dresden, Germany*

⁴*Institute for Functional Matter and Quantum Technologies,*

University of Stuttgart, Pfaffenwaldring 57, D-70569 Stuttgart, Germany

⁵*Max Planck Institute for Solid State Research, Heisenbergstrasse 1, D-70569 Stuttgart, Germany*

A range of honeycomb-lattice compounds has been proposed and investigated in the search for a topological Kitaev spin liquid. However, sizable Heisenberg interactions and additional symmetry-allowed exchange anisotropies in the magnetic Hamiltonian of these potential Kitaev materials push them away from the pure Kitaev spin-liquid state. Particularly the Kitaev-to-Heisenberg coupling ratio is essential in this respect. With the help of advanced quantum-chemistry methods, we explore how the magnetic coupling ratios depend on pressure in several honeycomb compounds (Na_2IrO_3 , $\beta\text{-Li}_2\text{IrO}_3$, and $\alpha\text{-RuCl}_3$). We find that the Heisenberg and Kitaev terms are affected differently by uniform pressure or strain: the Kitaev component increases more rapidly than the Heisenberg counterpart. This provides a scenario where applying pressure or strain can stabilize a spin liquid in such materials.

Introduction. The realization of quantum spin liquids (QSLs) in spin-orbit driven correlated materials is an intensively pursued goal in the condensed matter community, both experimentally and theoretically. In a QSL strong quantum fluctuations prevent long-range magnetic order even at the lowest temperatures and instead a non-trivial ground state forms with long-range quantum entanglement between spins [1–3]. Of particularly great promise in this context is the Kitaev Hamiltonian on honeycomb lattices, which exhibits various topological spin-liquid phases [4]. The paramount attention given to such states can be understood by the fact that they are topologically protected from decoherence [5], display fractional excitations with Majorana statistics, and therefore hold promise in the field of quantum information and quantum computation.

The quest for the physical realization of the Kitaev spin liquid for effectively spin-1/2 particles took a big stride forward with the proposal of the honeycomb $5d^5$ iridate materials as host of the Kitaev-Heisenberg model [6, 7]. The latter describes the interactions between spin-1/2 moments with the help of two competing nearest-neighbor (NN) couplings, i.e., an isotropic Heisenberg term (J) assumed to mainly arise from direct exchange between Ir-ion d orbitals and an anisotropic Kitaev component (K) which stems from superexchange along the Ir-O-Ir paths.

Certain materials, in particular Na_2IrO_3 , $\beta\text{-Li}_2\text{IrO}_3$, and $\alpha\text{-RuCl}_3$, have been extensively studied experimentally in this context [8–18] as well as within the electronic-structure computational field, by either quantum-chemistry [19–21] or density-functional-based [22–25] methods. However, it turns out that the anticipated spin-liquid regime is precluded in these honeycomb compounds, most likely due to the presence of reasonably strong Heisenberg interactions, longer-range spin cou-

plings, or the combination of both these factors. So far, all the measurements indicate magnetic long-range order at low temperatures and zero external magnetic field. None of these systems however exhibits the conventional Néel state although the magnetic ions form bipartite lattices in all of them. It has been suggested that these materials are still located in the phase diagram in close vicinity to the spin-liquid regime [12, 13, 15, 17, 18]. This has then inspired rigorous experimental effort to test their properties under strain or pressure [12, 26–28]. In particular, there have been claims for finding the evidences of spin-liquid states under applied pressure in $\beta\text{-Li}_2\text{IrO}_3$ [12, 26], $\gamma\text{-Li}_2\text{IrO}_3$ [27], and $\alpha\text{-RuCl}_3$ [28]. It is worth noting that even more complex strain experiments have been suggested [29, 30]. For $\alpha\text{-RuCl}_3$ indications for an emergent spin-liquid phase induced by magnetic field have also been observed [21, 31].

Here we explore the effects of pressure on the NN isotropic and anisotropic interactions by employing *ab initio* quantum-chemistry methods. In order to interpret the response of the magnetic exchange couplings under uniform pressure, we start by analysing the dependence of both the Kitaev and Heisenberg terms on the lattice constants. By adopting an idealised model in which under uniform pressure the lattice just scales down to a configuration with smaller unit-cell parameters, we obtain expressions which show that the Kitaev coupling constant increases more rapidly than the Heisenberg J , giving large K/J ratios for shorter bonds and thus an enhancement towards spin-liquid formation in the phase diagram of the Kitaev-Heisenberg model under volume change. The amplitude of this enhancement for the Kitaev term is also confirmed by *ab initio* quantum-chemistry calculations in the case of honeycomb compounds. However, in the case of hyperhoneycomb Li_2IrO_3 , in addition to the upsurge of Kitaev

exchange, the symmetric off-diagonal Γ couplings also become significantly larger and might play an important role in shaping its magnetic properties, as discussed in Ref. 32. Looking at such trends gives a profound insight into the different competing processes coming into play for different compounds or structures and can provide guidelines or direction for further experimental investigations.

Qualitative analysis. The Kitaev-Heisenberg Hamiltonian [7] originally proposed as a minimal model for the honeycomb-lattice iridates takes the following form on a given bond of NN's i, j :

$$\mathcal{H}_{ij}^{(\gamma)} = J \tilde{\mathbf{S}}_i \cdot \tilde{\mathbf{S}}_j + K \tilde{S}_i^\gamma \tilde{S}_j^\gamma, \quad (1)$$

where $\tilde{\mathbf{S}}_i$ and $\tilde{\mathbf{S}}_j$ represent pseudospin 1/2 operators for the ground-state Kramers doublets of Ir^{4+} (or Ru^{3+}) ions, the first and second terms correspond to the isotropic Heisenberg interaction and the anisotropic Kitaev coupling, respectively, and $\gamma \in \{x, y, z\}$ labels the three inequivalent bonds and the corresponding Cartesian components of the pseudospins. Depending on the K/J ratio, the model (1) is known to host a rich phase diagram containing the Kitaev spin-liquid and a variety of ordered states [7, 33].

To qualitatively understand pressure effects on the effective coupling constants K and J , we assume that under uniform pressure all inter-atomic distances rescale in the same way and consider only the leading contributions to the exchange interactions. A perturbative analysis estimates that $J \sim \frac{t_{dd}^2}{U}$ and $K \sim -\frac{t_{pd}^4}{\Delta_{pd}^2} \frac{J_H}{U^2}$ [6, 7], with the Heisenberg term predominantly related to direct exchange while the Kitaev interaction is mostly due to superexchange processes along the Ir-O-Ir paths. Here, t_{dd} and t_{pd} stand for the hybridisation amplitudes between d -orbitals of neighboring Ir ions and between Ir d and O p states, respectively, and Δ_{pd} is the charge-transfer energy. The interaction parameters U and J_H correspond to the on-site Coulomb repulsion and the Hund coupling, respectively. In the simplest picture, the hybridisation amplitudes scale with the inter-ionic distance r as $t_{dd} \sim r^{-5}$ and $t_{pd} \sim r^{-7/2}$ [34]. This, in turn, gives a rescaling of the coupling constants $J = J_0 \left(\frac{a}{a_0}\right)^{-10}$ and $K = K_0 \left(\frac{a}{a_0}\right)^{-14}$ when the characteristic inter-ionic length scale changes from a_0 to a under uniform pressure or strain.

The above naive estimates are based on the dominant subset of possible exchange processes and are thus rather rough in character. However, they do suggest that the strengths of the different NN isotropic and anisotropic coupling constants get differently renormalized under uniform pressure. In order to test this quantitatively we have performed electronic-structure calculations using many-body quantum-chemistry methods to rigorously

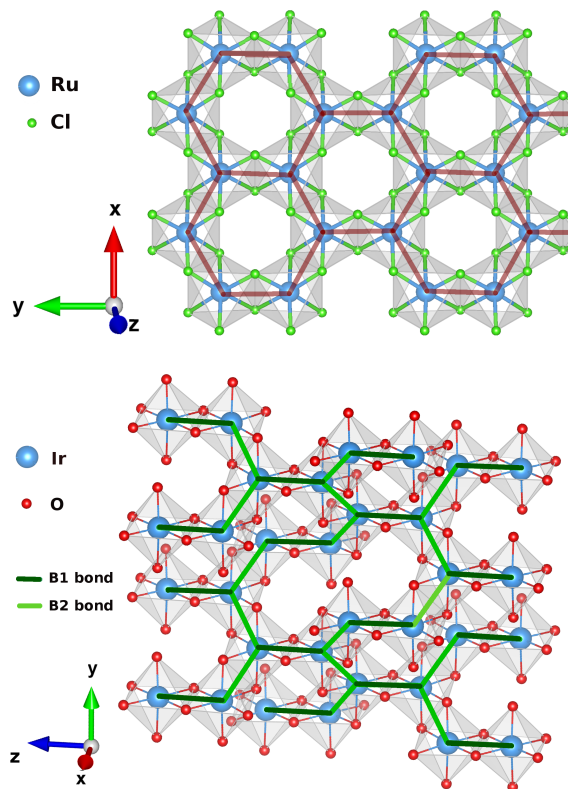


FIG. 1. (top) Ru-ion honeycomb lattice (blue) with Cl-ligand octahedral coordination (green sites) in RuCl_3 . (bottom) Ir-ion hyperhoneycomb lattice in $\beta\text{-Li}_2\text{IrO}_3$. The local environment of the Ir sites remains similar to the 2D honeycomb network shown above.

account for all symmetry-allowed NN exchange paths for variable inter-ionic distances within a family of potential Kitaev spin-liquid materials.

Electronic-structure calculations. The transition-metal (TM) ions, i.e., Ir/Ru, in the oxides and the chloride discussed here frame a honeycomb (Na_2IrO_3 and $\alpha\text{-RuCl}_3$) or hyperhoneycomb lattice ($\beta\text{-Li}_2\text{IrO}_3$), as shown in Fig. 1, where each site is connected to three TM NNs. The Ir ions in Na_2IrO_3 and $\beta\text{-Li}_2\text{IrO}_3$ have a 4+ oxidation state, which implies five $5d$ -shell electrons. The octahedral ligand (L) coordination makes that the $5d$ levels are split into e_g and t_{2g} states, with the latter lying at significantly lower energy [35]. Given the large $t_{2g}-e_g$ splitting, the five valence electrons enter the t_{2g} subshell in first approximation, which yields an effective picture of one hole within the t_{2g} sector. In the presence of strong spin-orbit coupling, this can be mapped onto a set of fully occupied $j_{\text{eff}} = 3/2$ and half-filled $j_{\text{eff}} = 1/2$ states [6, 36, 37]. Deviations from a perfect cubic environment may lead to admixture of these $j_{\text{eff}} = 1/2$ and $j_{\text{eff}} = 3/2$ components. The key structural difference between the honeycomb and hyperhoneycomb lattices is that the Ir ions frame a truly 2D network in the former

while they form a slightly more complicated 3D arrangement in the latter, with alternate rotation of two adjacent B2 bonds around the B1 link (see Fig 1(b)). However, the essential local environment of Ir is similar to the 2D honeycomb structure. The Ru ions in α -RuCl₃ have a 3+ oxidation state, which again implies five electrons in the (4*d*) valence shell. Similar to the 5*d* compounds, the ligand field splits the 4*d* levels into *t*_{2*g*} and *e*_{*g*} states. Spin-orbit coupling is significantly weaker for 4*d* orbitals, but still large enough to generate strongly spin-orbital entangled 1/2 pseudospins for moderate trigonal distortion [21].

In both Na₂IrO₃ and α -RuCl₃, the NN octahedra display *C*_{2*h*} point-group symmetry, which then allows a generalized bilinear Hamiltonian of the following form for a pair of pseudospins *i* and *j*:

$$\mathcal{H}_{ij}^{(\gamma)} = J \tilde{\mathbf{S}}_i \cdot \tilde{\mathbf{S}}_j + K \tilde{S}_i^\gamma \tilde{S}_j^\gamma + \sum_{\alpha \neq \beta} \Gamma_{\alpha\beta} (\tilde{S}_i^\alpha \tilde{S}_j^\beta + \tilde{S}_i^\beta \tilde{S}_j^\alpha), \quad (2)$$

where the $\Gamma_{\alpha\beta}$ coefficients refer to the off-diagonal components of the symmetric anisotropic exchange matrix, with $\alpha, \beta \in \{x, y, z\}$. An antisymmetric Dzyaloshinskii-Moriya (DM) exchange is not allowed, given the inversion center for the block of two NN octahedra.

On the other hand, a block of two NN octahedra in the hyperhoneycomb structure may display two different types of point-group symmetry: the so called B2 bonds have *C*_{2*h*} point-group symmetry and the Hamiltonian for these links is given by Eq. (2), while bond B1 displays

TABLE I. NN magnetic couplings (in meV) for bond B1 in Na₂IrO₃ as functions of variable Ir-Ir bond length *a*; the relative change is $\delta a = a/a_0 - 1$. Results of spin-orbit MRCI calculations are shown.

δa	<i>a</i> (Å)	<i>K</i>	<i>J</i>	Γ_{xy}	$\Gamma_{zx} = -\Gamma_{yz}$	$ K/J $
+2%	3.20	-16.9	4.0	-0.2	0.4	4.23
Exp.	3.14	-20.8	5.2	-0.7	0.8	3.98
-1.5%	3.09	-24.6	5.9	-1.3	1.1	4.13
-3%	3.04	-28.9	6.8	-2.3	1.5	4.27
-5%	2.98	-34.7	7.7	-3.4	2.1	4.50

TABLE II. NN magnetic couplings (in meV) for bond B2 in Na₂IrO₃ for variable Ir-Ir bond length *a*, results of spin-orbit MRCI calculations.

δa	<i>a</i> (Å)	<i>K</i>	<i>J</i>	Γ_{xy}	$\Gamma_{zx} = -\Gamma_{yz}$	$ K/J $
+2%	3.19	-12.0	0.9	-0.97	-0.61	11.89
Exp.	3.13	-15.6	2.2	-1.12	-0.84	7.07
-1.5%	3.08	-18.2	3.1	-1.43	-0.92	5.89
-3%	3.04	-21.0	3.7	-1.8	-1.3	5.56
-5%	2.97	-25.6	4.8	-2.5	-1.7	5.30

TABLE III. NN magnetic couplings (in meV) in RuCl₃ for variable Ru-Ru bond length *a*, results of spin-orbit MRCI calculations.

δa	<i>a</i> (Å)	<i>K</i>	<i>J</i>	Γ_{xy}	$\Gamma_{zx} = -\Gamma_{yz}$	$ K/J $
+2%	3.52	-4.1	0.8	-0.9	-0.4	5.31
Exp.	3.45	-5.6	1.2	-1.2	-0.7	4.67
-1.5%	3.40	-7.1	1.8	-1.3	-0.9	3.99
-3%	3.35	-8.7	2.3	-1.6	-1.2	3.78
-5%	3.28	-11.4	2.8	-2.0	-1.8	4.05

*D*₂ point-group symmetry and allows DM antisymmetric anisotropic exchange in the Hamiltonian [20]. However, only the *x*-component of the DM vector is non-zero. The Hamiltonian for bond B1 can be then written as:

$$\tilde{\mathcal{H}}_{ij}^{(z)} = J \tilde{\mathbf{S}}_i \cdot \tilde{\mathbf{S}}_j + K \tilde{S}_i^z \tilde{S}_j^z + \Gamma_{xy} (\tilde{S}_i^x \tilde{S}_j^y + \tilde{S}_i^y \tilde{S}_j^x) + \mathbf{D} \cdot \tilde{\mathbf{S}}_i \times \tilde{\mathbf{S}}_j. \quad (3)$$

A local Kitaev reference frame is used here, such that for each TM-TM link, the *z*-coordinate is perpendicular to the TM₂L₂ plaquette. Mapping of the *ab initio* data onto an effective spin Hamiltonian is carried out following the procedure earlier used in Refs. [21, 38, 39]. Experimental crystallographic data were used in the present calculations for Na₂IrO₃, β -Li₂IrO₃, and α -RuCl₃ as reported in [10, 12, 40], respectively. To test the qualitative trends found phenomenologically for the rescaling of the coupling constants, we further considered structural data corresponding to -1.5%, -3%, -5%, and +2% change in the TM-TM bond length in the many-body quantum-chemistry calculations. Further details of the calculations are provided in SM.

Results. We start our discussion on the variations of the magnetic exchange interactions when modifying bond lengths with the case of Na₂IrO₃. NN magnetic couplings as derived from spin-orbit multireference configuration-interaction (MRCI) calculations [41] are listed in Table I. For bond B1, *K* increases from -20.8 meV for to the experimental crystal structure at ambient pressure to -35.7 meV on 5% reduction of the Ir-Ir bond length. *J*, on the other hand, displays a rather modest enhancement, from 5.2 to 7.7 meV. This translates in an increase of the $|K/J|$ ratio from 3.98 to 4.50. Γ_{xy} and Γ_{zx} also gain significant strength with rising pressure but remain nevertheless one order of magnitude smaller than *K*.

In the case of bond B2, the trends look a bit different: while *K* evolves in a similar fashion as for bond B1, *J* becomes almost twice the value at ambient pressure for the shortest Ir-Ir bond length considered here. As a consequence, $|K/J|$ decreases for bond B2 (see Table II). However, the $|K/J|$ ratio jumps from 7 at ambient pressure to 12 for 2% elongation of the Ir-Ir bond. Such increased bond lengths could be realized under tensile strain. The

steep rise of the $|K/J|$ ratio can be understood as a result of the rapid downturn of the Heisenberg J towards 0. In fact, such a decreasing trend in J suggests that it would completely vanish with further slight elongation of the bonds, which then would lead to a Hamiltonian of pure anisotropic nature. The fact that the two distinct links in Na_2IrO_3 show different relative gain in K and J with the change in Ir-Ir distance indicates that the strength of the spin-spin couplings and various exchange processes for each bond are additionally significantly controlled by other attributes of the local environment such as the Ir-O-Ir angle.

The variations of the NN magnetic exchange interactions with modifying bond lengths in $\alpha\text{-RuCl}_3$, as obtained by spin-orbit MRCI calculations, are listed in Table III. K remains on the ferromagnetic side and increases to -11.5 meV on 5% reduction of the Ru-Ru distance as compared to the value of -5.6 meV at ambient pressure. For the same case, J moves to 2.8 meV from a value of 1.2 meV at normal pressure. An interesting point to note is again the reduction of J towards zero with 2% elongation of the Ru-Ru bond. For stretched bonds, the $|K/J|$ ratio reaches in fact the largest value. Γ_{xy} and Γ_{zx} also display a strong dependence on interatomic distances but these effective parameters are never larger than 25% of K in RuCl_3 . In contrast, in $\beta\text{-Li}_2\text{IrO}_3$, Γ_{xy} becomes as large as half the value of K and twice the value of J for the shortest Ir-Ir distance considered for bond B2 (see Tables IV and V). This large Γ_{xy} stands out while comparing trends with other honeycomb systems.

TABLE IV. NN magnetic couplings (in meV) for bond B1 in $\beta\text{-Li}_2\text{IrO}_3$ for variable Ir-Ir bond length a , results of spin-orbit MRCI calculations.

δa	a (Å)	K	J	D_x	Γ_{xy}
+2%	3.04	-11.70	0.21	0.30	-1.69
Exp.	2.98	-14.78	-0.26	0.35	-2.08
-3%	2.89	-17.01	-0.41	0.45	-3.48
-5%	2.83	-20.72	-0.60	0.56	-4.80

TABLE V. NN magnetic couplings (in meV) for bond B2 in $\beta\text{-Li}_2\text{IrO}_3$ for variable Ir-Ir bond length a , results of spin-orbit MRCI calculations.

δa	a (Å)	K	J	Γ_{xy}	$\Gamma_{zx} = -\Gamma_{yz}$	$ K/J $
+2%	3.03	-11.1	-0.9	-3.0	-0.7	11.85
Exp.	2.97	-12.2	-2.1	-4.1	-1.0	5.81
-1.5%	2.93	-14.1	-2.7	-4.9	-1.1	5.20
-3%	2.88	-15.6	-3.2	-6.1	-1.3	4.88
-5%	2.82	-17.7	-3.8	-8.1	-1.7	4.57

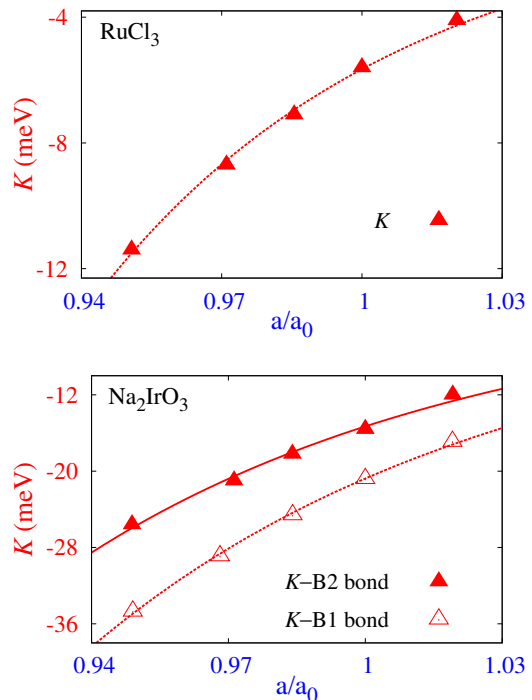


FIG. 2. NN Kitaev coupling for variable TM-TM bond length, fitted with the function $K = K_0 x^n$; plots for $\alpha\text{-RuCl}_3$ (top) and for B1 and B2 links in Na_2IrO_3 (bottom) are shown.

All NN magnetic couplings computed for $\beta\text{-Li}_2\text{IrO}_3$ are listed in Tables IV and V. For the case of B2 links in $\beta\text{-Li}_2\text{IrO}_3$, K rises to -17.7 meV on 5% cutback in the Ir-Ir distance, an increase by nearly 50% as compared to -12.2 meV at ambient pressure. J , on the other hand, changes from -2.1 meV at ambient conditions to a value of -3.8 meV. Similar to the other compounds, the $|K/J|$ ratio is maximum for positive bond-length increments. J even changes sign for 2% increase of the Ir-Ir distance for bond B1, which suggests that applying a very modest amount of tensile strain might bring the system close to the $J = 0$ limit, where only the anisotropic couplings are finite.

To determine the order of the exponential dependence of K as a function of changes in the TM-TM distance, the trends shown in the tables were fitted to the function $K = K_0 x^n$, where K_0 represents the Kitaev exchange amplitude at ambient pressure and n refers to the exponent of fractional change in the TM-TM distance, i.e., $a/a_0 = 1 + \delta a$. The plots shown in Fig. 2 display the variation of K in Na_2IrO_3 and $\alpha\text{-RuCl}_3$ fitted to such a function. Using these fits, the value of the exponent is determined to be $n = -15$ for the case of RuCl_3 . The exponent decreases to the values of $n = -13$ and -11 for the cases of the bonds B2 and B1 in Na_2IrO_3 , respectively, while it becomes as small as $n = -8$ for the Ir-Ir bonds in $\beta\text{-Li}_2\text{IrO}_3$. The value of the exponent for

α -RuCl₃ fits very nicely to the values predicted by the simplistic picture mentioned in the qualitative analysis section. The lower values of exponent obtained in the cases of Na₂IrO₃ and β -Li₂IrO₃ points to the changing nature of the exchange processes with slight modification of the surroundings, such as having different bond angles and ligand charge.

Summary. We have employed advanced quantum-chemistry methods to model the effects of uniform pressure and strain on the exchange couplings in iridium and ruthenium compounds with honeycomb and related lattices. The obtained results demonstrate that the Kitaev, Heisenberg, symmetric off-diagonal, and antisymmetric anisotropic magnetic interactions stemming from the different exchange processes renormalize differently under volume change. This, in turn, suggests that by introducing external pressure or strain on actual materials one could experimentally explore the extremely rich theoretical phase diagram composed of the quantum-spin liquid, collinear, as well as non-collinear ordered states. We believe that the present results are relevant to the pressure-induced melting of the magnetic long-range order experimentally suggested in β -Li₂IrO₃ and α -RuCl₃ compounds [12, 26, 28] and will motivate further pressure and strain experiments on Kitaev materials.

This work is supported by the DFG through SFB 1143. GJ, SR, and JvdB benefitted from the facilities of the KITP. GJ was supported in part by the NSF under Grant No. NSF PHY11-25915. RY and LH acknowledge Ulrike Nitzsche for technical support.

* Also at Andronikashvili Institute of Physics, 0177 Tbilisi, Georgia

- [1] L. Balents, “Spin liquids in frustrated magnets,” *Nature* **464**, 199–208 (2010).
- [2] T.-H. Han, J. S. Helton, S. Chu, D. G. Nocera, J. A. Rodriguez-Rivera, C. Broholm, and Y. S. Lee, “Fractionalized excitations in the spin-liquid state of a kagome-lattice antiferromagnet,” *Nature* **492**, 406–410 (2012).
- [3] M. Yamashita, N. Nakata, Y. Senshu, M. Nagata, H. M. Yamamoto, R. Kato, T. Shibauchi, and Y. Matsuda, “Highly Mobile Gapless Excitations in a Two-Dimensional Candidate Quantum Spin Liquid,” *Science* **328**, 1246–1248 (2010).
- [4] A. Kitaev, “Anyons in an exactly solved model and beyond,” *Ann. Phys.* **321**, 2 – 111 (2006).
- [5] S. M. Albrecht, A. P. Higginbotham, M. Madsen, F. Kuemmeth, T. S. Jespersen, J. Nygrd, P. Krogstrup, and C. M. Marcus, “Exponential protection of zero modes in Majorana islands,” *Nature* **531**, 206 (2016).
- [6] G. Jackeli and G. Khaliullin, “Mott Insulators in the Strong Spin-Orbit Coupling Limit: From Heisenberg to a Quantum Compass and Kitaev Models,” *Phys. Rev. Lett.* **102**, 017205 (2009).
- [7] J. Chaloupka, G. Jackeli, and G. Khaliullin, “Kitaev-Heisenberg Model on a Honeycomb Lattice: Possible Exotic Phases in Iridium Oxides A₂IrO₃,” *Phys. Rev. Lett.* **105**, 027204 (2010).
- [8] Y. Singh and P. Gegenwart, “Antiferromagnetic Mott insulating state in single crystals of the honeycomb lattice material Na₂IrO₃,” *Phys. Rev. B* **82**, 064412 (2010).
- [9] F. Ye, S. Chi, H. Cao, B. C. Chakoumakos, J. A. Fernandez-Baca, R. Custelcean, T. F. Qi, O. B. Korneta, and G. Cao, “Direct evidence of a zigzag spin-chain structure in the honeycomb lattice: A neutron and x-ray diffraction investigation of single-crystal Na₂IrO₃,” *Phys. Rev. B* **85**, 180403 (2012).
- [10] S. K. Choi, R. Coldea, A. N. Kolmogorov, T. Lancaster, I. I. Mazin, S. J. Blundell, P. G. Radaelli, Yogesh Singh, P. Gegenwart, K. R. Choi, S.-W. Cheong, P. J. Baker, C. Stock, and J. Taylor, “Spin Waves and Revised Crystal Structure of Honeycomb Iridate Na₂IrO₃,” *Phys. Rev. Lett.* **108**, 127204 (2012).
- [11] K. A. Modic, T. E. Smidt, I. Kimchi, N. P. Breznay, A. Biffin, S. Choi, R. D. Johnson, R. Coldea, P. Watkins-Curry, G. T. McCandless, J. Y. Chan, F. Gandara, Z. Islam, A. Vishwanath, A. Shekhter, R. D. McDonald, and J. G. Analytis, “Realization of a three-dimensional spin-anisotropic harmonic honeycomb iridate,” *Nat. Commun.* **5**, 4203 (2014).
- [12] T. Takayama, A. Kato, R. Dinnebier, J. Nuss, H. Kono, L.S.I. Veiga, G. Fabbri, D. Haskel, and H. Takagi, “Hyperhoneycomb Iridate β -Li₂IrO₃ as a Platform for Kitaev Magnetism,” *Phys. Rev. Lett.* **114**, 077202 (2015).
- [13] S. H. Chun, J.-W. Kim, J. Kim, H. Zheng, C. C. Stoumpos, C. D. Malliakas, J. F. Mitchell, K. Mehlawat, Y. Singh, Y. Choi, T. Gog, A. Al-Zein, M. M. Sala, M. Krisch, J. Chaloupka, G. Jackeli, G. Khaliullin, and B. J. Kim, “Direct evidence for dominant bond-directional interactions in a honeycomb lattice iridate Na₂IrO₃,” *Nat. Phys.* **11**, 462–466 (2015).
- [14] R. D. Johnson, S. C. Williams, A. A. Haghighirad, J. Singleton, V. Zapf, P. Manuel, I. I. Mazin, Y. Li, H. O. Jeschke, R. Valentí, and R. Coldea, “Monoclinic crystal structure of α -RuCl₃ and the zigzag antiferromagnetic ground state,” *Phys. Rev. B* **92**, 235119 (2015).
- [15] L. J. Sandilands, Y. Tian, K. W. Plumb, Y.-J. Kim, and K. S. Burch, “Scattering Continuum and Possible Fractionalized Excitations in α -RuCl₃,” *Phys. Rev. Lett.* **114**, 147201 (2015).
- [16] L. J. Sandilands, Y. Tian, Anjan A. Reijnders, Heung-Sik Kim, K. W. Plumb, Young-June Kim, Hae-Young Kee, and Kenneth S. Burch, “Spin-orbit excitations and electronic structure of the putative Kitaev magnet α -RuCl₃,” *Phys. Rev. B* **93**, 075144 (2016).
- [17] A. Banerjee, C. A. Bridges, J.-Q. Yan, A. A. Aczel, L. Li, M. B. Stone, G. E. Granroth, M. D. Lumsden, Y. Yiu, J. Knolle, S. Bhattacharjee, D. L. Kovrizhin, R. Moessner, D. A. Tennant, D. G. Mandrus, and S. E. Nagler, “Proximate Kitaev quantum spin liquid behaviour in a honeycomb magnet,” *Nat. Mater.* **4604** (2016).
- [18] A. Banerjee, J. Yan, J. Knolle, C. A. Bridges, M. B. Stone, M. D. Lumsden, D. G. Mandrus, D. A. Tennant, R. Moessner, and S. E. Nagler, “Neutron scattering in the proximate quantum spin liquid α -RuCl₃,” *Science* **356**, 1055–1059 (2017).
- [19] V. M. Katukuri, S. Nishimoto, V. Yushankhai, A. Stoyanova, H. Kandpal, S. Choi, R. Coldea, I. Rousochatzakis, L. Hozoi, and J. van den Brink, “Kitaev interactions between $j = 1/2$ moments in honeycomb Na₂IrO₃ are

- large and ferromagnetic: insights from ab initio quantum chemistry calculations,” *New J. Phys.* **16**, 013056 (2014).
- [20] V. M. Katukuri, R. Yadav, L. Hozoi, S. Nishimoto, and J. van den Brink, “The vicinity of hyper-honeycomb β - Li_2IrO_3 to a three dimensional Kitaev spin liquid state,” *Sci. Rep.* **6**, 29585 (2016).
- [21] R. Yadav, N. A. Bogdanov, V. M. Katukuri, S. Nishimoto, J. van den Brink, and L. Hozoi, “Kitaev exchange and field-induced quantum spin-liquid states in honeycomb α - RuCl_3 ,” *Sci. Rep.* **6**, 37925 (2016).
- [22] J. G. Rau, Eric K.-H. Lee, and H.-Y. Kee, “Generic Spin Model for the Honeycomb Iridates beyond the Kitaev Limit,” *Phys. Rev. Lett.* **112**, 077204 (2014).
- [23] Y. Yamaji, Y. Nomura, M. Kurita, R. Arita, and M. Imada, “First-Principles Study of the Honeycomb-Lattice Iridates Na_2IrO_3 in the Presence of Strong Spin-Orbit Interaction and Electron Correlations,” *Phys. Rev. Lett.* **113**, 107201 (2014).
- [24] H.-S. Kim, V. Shankar, A. Catuneanu, and H.-Y. Kee, “Kitaev magnetism in honeycomb RuCl_3 with intermediate spin-orbit coupling,” *Phys. Rev. B* **91**, 241110 (2015).
- [25] S. M. Winter, A. A. Tsirlin, M. Daghofer, J. van den Brink, Y. Singh, P. Gegenwart, and R. Valenti, “Models and materials for generalized Kitaev magnetism,” *J. Phys. Condens. Matter* **29**, 493002 (2017).
- [26] L. S. I. Veiga, M. Etter, K. Glazyrin, F. Sun, C. A. Escanhoela, G. Fabbri, J. R. L. Mardegan, P. S. Malavi, Y. Deng, P. P. Stavropoulos, H.-Y. Kee, W. G. Yang, M. van Veenendaal, J. S. Schilling, T. Takayama, H. Takagi, and D. Haskel, “Pressure tuning of bond-directional exchange interactions and magnetic frustration in the hyperhoneycomb iridate β - Li_2IrO_3 ,” *Phys. Rev. B* **96**, 140402 (2017).
- [27] N. P. Breznay, A. Ruiz, A. Frano, W. Bi, R. J. Birgeneau, D. Haskel, and J. G. Analytis, “Resonant x-ray scattering reveals possible disappearance of magnetic order under hydrostatic pressure in the Kitaev candidate γ - Li_2IrO_3 ,” *Phys. Rev. B* **96**, 020402 (2017).
- [28] Z. Wang *et al.*, “Observation of the quantum spin liquid state in pressurized α - RuCl_3 ,” arxiv:1705.06139 (2017).
- [29] S. Rachel, L. Fritz, and M. Vojta, “Landau levels of Majorana fermions in a spin liquid,” *Phys. Rev. Lett.* **116**, 167201 (2016).
- [30] B. Perreault, S. Rachel, F. J. Burnell, and J. Knolle, “Majorana Landau-level Raman spectroscopy,” *Phys. Rev. B* **95**, 184429 (2017).
- [31] S.-H. Baek, S.-H. Do, K.-Y. Choi, Y. S. Kwon, A. U. B. Wolter, S. Nishimoto, Jeroen van den Brink, and B. Büchner, “Evidence for a field-induced quantum spin liquid in α - RuCl_3 ,” *Phys. Rev. Lett.* **119**, 037201 (2017).
- [32] I. Rousochatzakis and N. B. Perkins, “Classical spin liquid instability driven by off-diagonal exchange in strong spin-orbit magnets,” *Phys. Rev. Lett.* **118**, 147204 (2017).
- [33] J. Chaloupka, G. Jackeli, and G. Khaliullin, “Zigzag magnetic order in the iridium oxide Na_2IrO_3 ,” *Phys. Rev. Lett.* **110**, 097204 (2013).
- [34] W. A. Harrison, *Electronic Structure and the Properties of Solids: The Physics of the Chemical Bond* (Dover Publications, INC., NY, 1989).
- [35] H. Gretarsson, J. P. Clancy, X. Liu, J. P. Hill, Emil Bozin, Yogesh Singh, S. Manni, P. Gegenwart, Jungho Kim, A. H. Said, D. Casa, T. Gog, M. H. Upton, Heungsik Kim, J. Yu, Vamshi M. Katukuri, L. Hozoi, Jeroen van den Brink, and Young-June Kim, “Crystal-field splitting and correlation effect on the electronic structure of A_2IrO_3 ,” *Phys. Rev. Lett.* **110**, 076402 (2013).
- [36] A. Abragam and B. Bleaney, *Electron Paramagnetic Resonance of Transition Ions* (Clarendon Press, 1970).
- [37] B. J. Kim, Hosub Jin, S. J. Moon, J.-Y. Kim, B.-G. Park, C. S. Leem, Jaejun Yu, T. W. Noh, C. Kim, S.-J. Oh, J.-H. Park, V. Durairaj, G. Cao, and E. Rotenberg, “Novel $J_{\text{eff}} = 1/2$ Mott state induced by relativistic spin-orbit coupling in Sr_2IrO_4 ,” *Phys. Rev. Lett.* **101**, 076402 (2008).
- [38] N. A. Bogdanov, V. M. Katukuri, J. Romhányi, V. Yushankhai, V. Kataev, B. Büchner, J. van den Brink, and L. Hozoi, “Orbital reconstruction in nonpolar tetravalent transition-metal oxide layers,” *Nat. Commun.* **6**, 7306 (2015).
- [39] R. Yadav, M. Pereiro, N. A. Bogdanov, S. Nishimoto, A. Bergman, O. Eriksson, J. van den Brink, and L. Hozoi, “Heavy-mass magnetic modes in pyrochlore iridates due to dominant Dzyaloshinskii-Moriya interaction,” arxiv:1707.00500 (2017).
- [40] H. B. Cao, A. Banerjee, J.-Q. Yan, C. A. Bridges, M. D. Lumsden, D. G. Mandrus, D. A. Tennant, B. C. Chakoumakos, and S. E. Nagler, “Low-temperature crystal and magnetic structure of α - RuCl_3 ,” arXiv:1602.08112 (2016).
- [41] T. Helgaker, P. Jørgensen, and J. Olsen, *Molecular Electronic-Structure Theory* (Wiley, Chichester, 2000).